

## Model for simulation of the sea salt aerosol atmospheric cycle

*S. Nickovic, ICoD, University of Malta; now at: World Meteorological Organization, Geneva, Switzerland;  
Z.I. Janjic, NCEP, Washington DC, USA; P. Kishsha and P. Alpert, Tel-Aviv University, Israel;  
email: snickovic@wmo.org*

There is an increasing interest in simulating various impacts of sea salt on the atmosphere, such as direct radiation effects and indirect effects on cloud formation. Sea salt aerosol is produced over the air-sea interface as a result of the air momentum transfer to the sea surface. The sea salt atmospheric process starts when strong winds generate whitecaps of the breaking waves with a high concentration of bubbles. Their bursting releases salt aerosol into the marine boundary layer. Once injected into the atmosphere, the sea salt is transported vertically and horizontally and it is deposited on the ground by wet and dry deposition.

In this article we describe a model for simulating the sea salt aerosol atmospheric cycle. This model (DREAM-SALT) is based on the DREAM dust aerosol model (Nickovic et al., 2001), which was adapted to function for sea salt aerosol. The NCEP/Eta regional atmospheric model (Janjic, 1994; Janjic, 2001; and references therein) drives the aerosol. The aerosol emission scheme is based on the viscous sublayer model (Janjic, 1994) in which energy and mass transfers above the air-sea interface critically depend on turbulent conditions. The Janjic viscous sublayer scheme is based on the following assumptions: (a) there are two distinct layers: a thin viscous sublayer immediately above the surface, and a turbulent layer above the viscous sublayer; (b) at the top of the viscous sublayer all fluxes are continuous. In the viscous sublayer, it is assumed that (1) the vertical transport is determined entirely by the molecular diffusion; and (2) vertical profiles of variables are linear since the viscous diffusivity is assumed to be constant. In the turbulent layer, the vertical transport is entirely defined by turbulent fluxes.

Depending on the Reynolds roughness number  $Re = z_0 u_* / \nu$ , the viscous sublayer scheme is assumed to operate in three different regimes: smooth and transitional; rough; and rough with spray. Here,  $z_0$ ,  $u_*$  and  $\nu$  are the roughness height, friction velocity and the air viscosity, respectively. When  $Re$  exceeds a prescribed critical value  $Re_c$ , the flow ceases to be smooth and enters the rough regime. The rough regime is characterized by combined viscous and turbulent mixing. In the rough regime with spray, the mixing becomes fully turbulent. Here, the breaking waves provide a mass exchange, which is more effective than that of the two previous regimes. The values of  $u_*$  at which the transitions between the different regimes occur are  $u_{*r} = 0.225 \text{ ms}^{-1}$  and  $u_{*s} = 0.7 \text{ ms}^{-1}$ .

Following Janjic (1994), the sea salt fluxes are defined by

$$F_{C(VSC)} = \nu \frac{C_{INT} - C_S}{z_{INT}}; \quad , \quad F_{C(TRB)} = K_C \frac{C_{LM} - C_{INT}}{z_{LM} - z_{INT}}$$

in the viscous and turbulent sublayers, respectively. Here,  $K_C$  is the Monin-Obukhov bulk turbulent mixing coefficient;  $C_S$ ,  $C_{INT}$  and  $C_{LM}$  are sea salt concentrations at the sea surface, at the top of the viscous sublayer and at the first computational model layer, respectively;  $z_{INT}$  and  $z_{LM}$  are the heights of the top of the viscous sublayer and the first computational model layer, respectively. The depth of the viscous sublayer is calculated as

$$z_{INT} = \frac{0.35M \sqrt[4]{R_r} \sqrt[2]{S_c} \nu}{u_*}$$

(Janjic, 1994). Here,  $S_c$  is the Schmidt number; the constant  $M$  has the value of 30 in the first regime and 10 in the second regime. The viscous sublayer depth  $z_{INT}$  decreases as the turbulence increases. The viscous sublayer vanishes in the last, rough regime with spray. From the requirement for continuity of the viscous and turbulent fluxes at the viscous/turbulent interface, it follows that  $C_{INT} = \frac{C_S + \omega C_{LM}}{1 + \omega}$ , where  $\omega = \frac{K_C z_{INT}}{\nu(z_{LM} - z_{INT})}$ . Here

$\omega$  plays the role of a weighting factor. Note that  $\omega$  vanishes with the disappearance of the viscous sublayer in the rough regime with spray. As a consequence, it follows that  $C_{INT} = C_S$  at  $z = z_0$ . In the Janjic scheme, the interface value  $C_{INT}$  is considered as the lower boundary condition for the surface turbulent scheme in the NCEP/Eta model.

In our approach, the aerosol concentration at the top of the viscous sublayer is used as the lower boundary condition, in contrast to most other sea salt models that use a flux form for the emission function (e.g. Monahan, 1986; Gong et al., 2003). In our ‘concentration’ boundary condition approach, effects of the viscous sublayer model are fully taken into account. Based on such concept, we have developed two alternate emission schemes.

The *first emission scheme* defines the lower boundary condition using the source function of Erickson et al. (1986):

$$C_S^j = 10^{-9} \alpha^j \exp(0.16U_{10} + 1.45) \quad \text{for } U_{10} \leq 15 \text{ ms}^{-1}; \quad j = 1, N$$

$$C_S^j = 10^{-9} \alpha^j \exp(0.13U_{10} + 1.89) \quad \text{for } U_{10} > 15 \text{ ms}^{-1}; \quad j = 1, N$$

Here,  $U_{10}$  is the 10m wind intensity;  $\alpha_j \in (0,1)$  is an array describing the source particle size distribution. In our model setup, we use  $N = 8$  particle categories with sizes ranging from 1-8  $\mu\text{m}$ . All variable units are given in the MKS system.

In the *second emission scheme*, the sea salt concentration on the top of the viscous sublayer is used as the lower boundary condition. It is assumed here that  $C_{INT}$  is proportional to the salinity of the predicted specific humidity  $q_{INT}$  at the same height:

$$C_{INT}^j = 10^{-3} \alpha^j S q_{INT} \rho_{air}$$

where,  $S$  is the sea water salinity;  $\rho_{air}$  is the air density. Again, variable units are in the MKS system.

Preliminary experiments with the sea salt model based on real-time atmospheric forecasts indicate that both emission schemes proposed in this study reproduce major observed features of sea salt aerosol, such as horizontal and vertical concentration distribution. Figure 1 shows 24-hour predicted horizontal distributions of surface sea-salt concentration and wind at 3000 m over the Mediterranean region on August 2, 2006. In Figure 2, time evolution of the sea salt concentration over the sea near the west coast of Africa is displayed. More extensive tests in the future will demonstrate which of the two proposed schemes more accurately simulate the sea salt process.

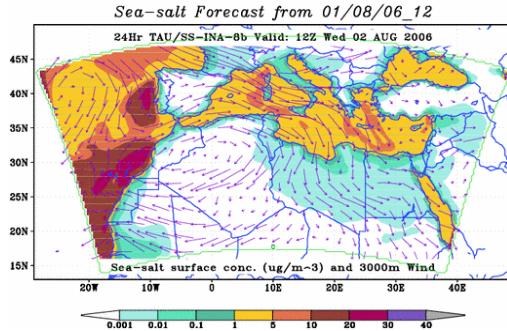


Fig. 1.

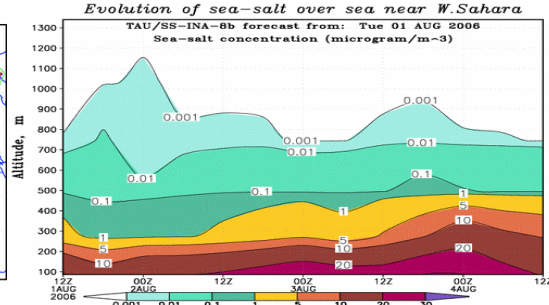


Fig. 2.

## ACKNOWLEDGEMENT

Major developments of the aerosol transport component were performed within the 4<sup>th</sup> Italo-Maltese Protocol (1995-2000).

## REFERENCES

- Gong, S.L., A parameterization of sea-salt aerosol source function for sub- and super- micron particles, *Global Biogeochemical Cycles*, 17 (4), 1097, doi:1029/2003GB002079, 2003.
- Janjic, Z. I., 1994: The step-mountain eta coordinate model: further developments of the convection, viscous sublayer and turbulence closure schemes. *Monthly Weather Review*, Vol. **122**, 927-945.
- Janjic, Z. I., 2001a: Nonsingular Implementation of the Mellor-Yamada Level 2.5 Scheme in the NCEP Meso model. NOAA/NWS/NCEP Office Note #437, December 2001, 61 pp.
- Nickovic, S., G. Kallos, A. Papadopoulos and O. Kakaliagou, 2001, A model for prediction of desert dust cycle in the atmosphere, *J. Geophys. Res.*, 106, 18113-18129.
- Monahan, E. C., D. E. Spiel, and K. L. Davidson, A model of marine aerosol generation via whitecaps and wave disruption, in *Oceanic Whitecaps and Their Role in Air-Sea Exchange*, edited by E. C. Monahan and G. Mac Niocaill, pp. 167-174, D. Reidel, Norwell, Mass., 1986.